Computing and Informatics, Vol. 42, 2023, 234–256, doi: 10.31577/cai_2023_1_234

COMPUTING ASPECTS OF SIMULATION BASED ON CONSERVATION LAWS CONDUCTED ON HPC CLUSTER

Peter Weisenpacher, Lukas Valasek, Jan Glasa

Institute of Informatics
Slovak Academy of Sciences
Dúbravská cesta 9
845 07 Bratislava, Slovakia
e-mail: {upsyweis, lukas.valasek, glasa.ui}@savba.sk

Abstract. The large amount of computing resources required for the simulation of complex natural processes demands a thorough analysis of the efficiency of the calculations and the conditions that influence it. This study investigates computing aspects of fire simulation conducted on a compute cluster. Current fire simulators based on principles of computational fluid dynamics are capable to realistically model majority of complex phenomena related to fire. Fire simulations are highly computationally demanding itself, however, they often lead to extensive parametrical studies requiring high performance computing systems. Smoke stratification and visibility during fire in a road tunnel with two emergency lay-bys are investigated by parametrical study comprising of 24 fire scenarios with the tunnel geometry modifications and various heat release rates and fire locations. Main tendencies of smoke spread in the downstream lay-by are identified and their mutual interactions are analysed. The simulation efficiency of particular simulations is analysed and the reasons of their varied elapsed times are investigated. The analysis indicates that the main reason of this variability are different jet fans velocities influenced by simulation scenario settings.

Keywords: Compute cluster, HPC, fire dynamics simulator, tunnel fire, smoke stratification

1 INTRODUCTION

The computational complexity of computer simulation systems solving many practical problems requires the use of considerable computing resources. In many cases, it is influenced by input parameters of the problem, which significantly affect the elapsed time and necessary computing resources. In addition, examining the influence of individual parameters of the investigated problem often requires the execution of a series of simulations differing from each other by the value of a specific input parameter the influence of which is the subject of research. Such parametric studies further increase the computational demands. Knowledge of the influence of individual input parameters of simulation on the elapsed time makes it possible to significantly optimize the deployment of available resources. Computational demands are particularly high in the case of simulation of physical processes described by conservation laws, including hydrology, design of jet engines, aerodynamics, fire simulations, etc. An example of the latter application is the globally used FDS (Fire Dynamics Simulator) code [1, 2]. One of its possible applications, requiring particularly high computational demands, is the simulation of fires in tunnels. The scope of these requirements is determined by the large size of computational domain involving a large-scale underground structure, the variability of its geometry, as well as the physical dynamics of the interaction of fire and air flows induced by jet fans. Parallel aproach is usually neccessary to tackle such problems. In this case, knowledge of the effect of individual input parameters on the elapsed time, and therefore also on the expected calculation requirements, is particularly important.

FDS (Fire Dynamics Simulator) [1, 2] is a CFD-based widely used simulation system for modelling fire and fire-driven fluid flows which was developed by NIST (National Institute of Standards and Technology, USA) in cooperation with the VTT (Technical Research Centre of Finland). FDS numerically solves a form of conservation equations for low-speed thermally-driven flows with an emphasis on smoke and heat transport from fire. The basic set of equations includes conservation equations for mass, species, momentum and energy:

$$\frac{\partial \rho}{\partial t} + \nabla . \rho \, \mathbf{u} = \dot{m}_b^{'''}, \tag{1}$$

$$\frac{\partial}{\partial t}(\rho Y_\alpha) + \nabla . \rho Y_\alpha \, \mathbf{u} = \nabla . \rho D_\alpha \nabla Y_\alpha + \dot{m}_\alpha^{'''} + \dot{m}_{b,\alpha}^{'''}, \tag{2}$$

$$\frac{\partial}{\partial t}(\rho \, \mathbf{u}) + \nabla . \rho \, \mathbf{u} \, \mathbf{u} + \nabla p = \rho + \mathbf{f}_b + \nabla . \tau_{ij}, \tag{3}$$

$$\frac{\partial}{\partial t}(\rho \, \mathbf{h}_s) + \nabla . \rho h_s \, \mathbf{u} = \frac{Dp}{Dt} + \dot{q}^{'''} - \dot{q}_b^{'''} - \nabla . \dot{q}^{''} + \varepsilon, \tag{4}$$

where $\dot{m}_b^{'''} = \sum_\alpha \dot{m}_{b,\alpha}^{'''}$ is the production rate of species by evaporating droplets or particles; ρ is the density; $\mathbf{u} = (u, v, w)$ is the velocity vector; Y_α, D_α, and $\dot{m}_{b,\alpha}^{'''}$ are the mass fraction, diffusion coefficient, and the mass production rate of α-th species per unit volume, respectively; p is the pressure; $\mathbf{f}_b$ is the external force vector; τ_{ij} is the viscous stress tensor; $\mathbf{h}_s$ is the sensible enthalpy; and $\mathbf{g}$ is the acceleration of gravity. The term $\dot{q}'''$ is the heat release rate per unit volume from a chemical reaction and $\dot{q}_b'''$ is the energy transferred to the evaporating droplets. The term $\dot{q}''$ represents the conductive and radiative heat fluxes. Note that $D()/Dt = \partial()/\partial t + \mathbf{u}.\nabla()$. To these four equations, the equation of state for a perfect gas

$$p = \frac{\rho R T}{\bar{W}}, \tag{5}$$

in which R is the universal gas constant, T is the temperature and $\bar{W}$ is the molecular weight of gas mixture, is added.

The core algorithm is an efficient explicit predictor-corrector scheme which is second order accurate in space and time. High efficiency of numerical methods implemented in FDS is redeemed by necessity of several simplifications causing specific limitations of the code. One of such limitations is relatively limited capabilities for geometry representation. The whole scene in which a fire is to be modelled, i.e., the size and shape of compartments and all relevant objects, must conform to rectangular numerical meshes required by FDS. FDS also includes numerous additional sub-models corresponding to all relevant fire related processes such as turbulence, thermal radiation and conductive heat transfer, pyrolysis and combustion of the pyrolysis products, etc. In FDS, several specific more sophisticated tools related to selected fire engineering applications are implemented such as the HVAC (Heating, Ventilation, and Air Conditioning) solver, sprinklers, various detectors and measuring devices, etc. FDS is widely used for fire engineering applications such as smoke movement and smoke handling systems in buildings and compartments [3, 4, 5, 6, 7], car parks [8, 9, 10], mines [11] and automobile fires [9, 12]. It is primarily used for solving practical problems in fire engineering; however, it can be used also to study fundamental fire dynamics in various environments [1]. Starting with FDS 6, the OpenMP model is employed by default. OpenMP (Open Multi-Processing) [13] is a programming interface that enables FDS to exploit multiple processing units (multiple cores) on a given computer. There are two ways of running the FDS in parallel: to exploit multiple cores on a single computer or to use multiple cores distributed over multiple computers on a network or compute cluster. The first way is the OpenMP which allows a single computer to run a single or multiple mesh FDS simulation on multiple cores. The use of OpenMP does not require decomposing the computational domain into multiple meshes, but it is able to work with simulations that have multiple meshes defined. The second way is based on an MPI (Message Passing Interface) [14], where the computational domain is divided into multiple meshes and typically each mesh is assigned to its own process. A multi-mesh FDS job is executed such that the flow field in each mesh is computed as an MPI process. MPI handles the transfer of information between the MPI processes (meshes). Each individual MPI process has its own independent memory. MPI and OpenMP can be used together; however, most of the speed up is achieved by the MPI model. In this study, the MPI model is chosen due to its high efficiency. Such parallelisation enables to deal with significant computational requirements of simulation and is necessary for modelling of fires in large structures.

Road tunnels belong to the important structures where the safe operation is absolutely vital to ensure safe transportation infrastructure. Fire in a tunnel is considered as significant emergency which can lead to enormous damages with consequences exceeding national or regional levels. Due to specific tunnel geometry, the gross amount of flammable materials being transported through the tunnel (vehicles and cargo) and a large number of passengers, such fire can become catastrophic with numerous victims and injured. Therefore, national and international authorities pay a particular attention to publishing safety precautions and regulations in order to improve the tunnel fire safety. Road tunnels in operation are equipped with various safety systems which are intended for early detection, localization and surveillance of fire and its development as well as by systems which are tasked to create and maintain suitable conditions for safe evacuation of tunnel users. One of such key safety systems is emergency ventilation prescribed for majority of medium and long road tunnels. Depending on the tunnel type, the aim of emergency ventilation in the case of fire is to achieve a prescribed target velocity of longitudinal airflow in the tunnel within a short prescribed time period and then to maintain it long enough to ensure safe evacuation of people. It is widely accepted that such proper airflow velocity can maintain smoke stratification in bi-directional road tunnels and prevent the descent of smoke from the upper part of the tunnel down to the head level and then to the roadway for a sufficiently long time. The concept of smoke stratification [15, 16, 17] is used in the strategy of ventilation operation applied in the case of fire not only in tunnels but also in various types of large structures such as atriums, large corridors and car parks [18, 19, 20]. CFD (Computational Fluid Dynamics) techniques are frequently used for the design and testing of ventilation systems as well as for computer simulation of fire and smoke propagation.

In the literature, only a limited number of full-scale tunnel validation studies can be found [3, 21, 22, 23]. It is partly because of the extremely simple spatial representation of tunnels and physical objects which does not support any curved or rounded shapes. All shapes must conform to rectilinear computational meshes required by FDS. This limits capabilities of FDS to model some specific features of the tunnel geometry such as frequently used tunnel curving, horseshoe tunnel cross-section, rounded jet fans, etc. In order to increase practitioners' and researchers' confidence in the FDS capability to capture tunnel airflows, an averaged air flow velocity and velocity profile were determined and compared against on-site measurements in the Dartford Tunnel (UK) [24]. The tunnel is 1 200 m long and 8.5 m in diameter. Even though the round tunnel cross-section was modelled as squared, the results correlated well with the measurements, indicating the FDS capability to simulate jet fans and airflows they generate. In [25, 26] the air flows generated by a jet fan in a big rectangular enclosure were studied experimentally and modelled by FDS 4 and FDS 6 to test novel developments in FDS 6 related to the turbulence model.

Several experimental and numerical studies dealt with various aspects of smoke stratification [27, 28, 19]. In [29] model scale tests and full-scale tests were used to establish correlations between gas temperature distribution and smoke stratification for tunnel applications. The investigated correlations are based on excess gas temperature ratios and Froude number scaling. In [30] the relationship between the longitudinal velocity and smoke stratification was explored and a proper velocity range that can maintain the downstream stratification was obtained. Based on Newman‘s theory, the "stratification velocity" is proposed, which is the maximum velocity that maintains downstream smoke stratification. In [31] the effects of water spray on the smoke stratification stability in the vicinity of a fire source were studied numerically. In [32] the effect of an upstream blockage on the thermal buoyant flow stratification in tunnel fires with longitudinal imposed airflow was revealed.

Designing the proper strategy of ventilation operation maintaining the smoke stratification in road tunnels is not a trivial task. Stratification can be strongly influenced by specific geometry of a particular tunnel, fire source location, heat release rate (HRR), piston effect and other factors. An important part of the tunnel geometry are emergency lay-bys which allow drivers to stop vehicles inside the tunnel without blocking traffic. Typically, they are located once in every 1 000 m of each tunnel lane [33]. Moreover, emergency evacuation exits are usually located in lay-bys, what makes them especially important for the smoke stratification research. Another crucial feature of the tunnel geometry is the tunnel inclination.

In the paper [34] the FDS 6 code ability to simulate the airflows generated by jet fans in a real road tunnel was studied. A transient model of the bi-directional medium length highway Polana tunnel [35] with horseshoe cross-section with longitudinal ventilation was created including details of the tunnel geometry as two emergency lay-bys, four pairs of axial jet fans and traffic signs. The developed model was calibrated to represent some details of the tunnel geometry which cannot be represented directly due to the chosen rectilinear computational mesh with 30 cm resolution such as the tunnel curving, objects with sub-grid dimensions, etc. The simulation results were in a good accordance with experimental data obtained during full-scale ventilation tests in the Polana tunnel [36].

In [37, 38] the influence of lay-bys on smoke spread in the same road tunnel was investigated using the model from [34]. Four geometrical variants of the tunnel were considered. Two different slopes of the tunnel, i.e., horizontal and sloping tunnels, were used. In addition to the real tunnels with two lay-bys, the corresponding fictional tunnels without lay-bys were also examined to determine the influence of lay-bys on smoke stratification. The smoke movement was simulated for three values of HRR and the influence of the lay-bys, slope and HRR on smoke stratification was evaluated using FDS 6. The visibility at the head level was used as a measure of smoke stratification. Two fire source locations (in the middle between the lay-bys and near the first lay-by) were considered.

This study continues in this research, summarizing and extending the findings from [37, 38], and discusses the simulations efficiency. As the visibility in the region of the lay-by located upstream was studied in [37, 38] thoroughly, the work is focused on more complex behaviour of fire smoke in the downstream lay-by and its vicinity. The influence of the tunnel slope, HRR and the existence/non-existence of the lay-bys on the smoke stratification in this region is studied. As three dimensional CFD simulations of fire in large compartments are very time consuming for fine mesh resolutions, this paper specifically focuses on analysis of elapsed real times of the simulations and their relation with the studied fire scenario parameters.

2 TUNNEL FIRE SCENARIOS

The considered tunnel (Figure 1) is 900 m long with a horseshoe cross section of dimensions 10.8 m (width) and 6.8 m (height). Two lay-bys; Lay-by I and Lay-by II, are located at 373 m (left side) and 635.6 m (right side) from the left (west) tunnel portal, respectively. The lay-by niches are 50 m long and 2.2 m wide with the maximal height of vaulted ceiling of 7.8 m. Such tunnel dimensions are frequently used in road tunnels in Slovakia [39, 40]. The geometry of the tunnel is modelled to conform into rectangular computational grid. Walls and road are represented by obstructions with material properties of two kinds of concrete [34]. The computational domain size is $900\,\mathrm{m} \times 18\,\mathrm{m} \times 8\,\mathrm{m}$ for all considered tunnels. The 20 cm mesh resolution used in the simulation allows significant simulations accuracy [34] at the expense of considerable elapsed times. The domain consists of $4\,500 \times 90 \times 40$ cells; the total number of cells is 16 200 000.

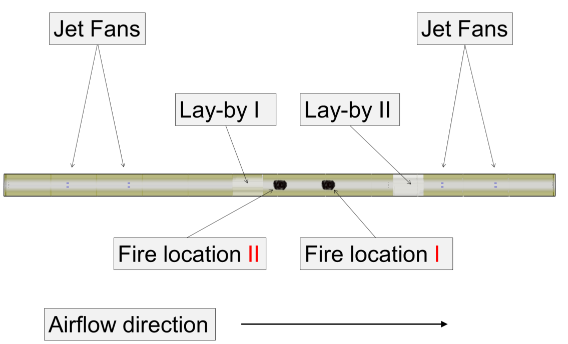

Figure 1. Tunnel scheme

Two Fire locations I and II were investigated; 529 m [37] and 453 m [38], respectively for three HRR values: 3 MW, 5 MW and 12 MW, corresponding to fires of a small passenger car, a large passenger car and a truck, respectively. Fire location I is located in the middle between both lay-bys. The Fire location II near the first lay-by was chosen for investigation of the spread of smoke through the whole section of the tunnel between both lay-bys and subsequent spread of cooled smoke in the second lay-by. The fire HRR increases linearly since the beginning of the simulation reaching its maximal value after 40 s to the fire. The fire source is represented by a VENT of dimensions $1\,\mathrm{m} \times 3\,\mathrm{m}$ located at the exact distance from the left tunnel portal. (Note that the words with capitals are the FDS names of the namelist groups, i.e., words used for description of fire scenario parameters in FDS input file.) The required HRR is achieved by a corresponding HRR per unit area (HRRPUA) prescribed to the VENT. The considerable high fire soot yield of 0.2 is set.

Four pairs of jet fans located at 101 m, 201 m, 716 m and 801 m are modelled by the HVAC feature of FDS 6. Rotor of jet fan is modelled by an obstruction of dimensions $0.6\,\mathrm{m} \times 0.8\,m$, 0.2 m thick. Two rectangular VENTs attached to it, with a prescribed normal velocity are used to model its inlet and outlet. The jet fan shroud is formed of four obstructions of the length of 3.8 m. The maximal volume flow is 18.62 $\mathrm{m}^3.\mathrm{s}^{-1}$. The jet fans operation is modelled via the RAMP feature, which is used for definition of dependent quantities in FDS.

Air velocity in the tunnel at the beginning of simulation is of $0\,\mathrm{m.s}^{-1}$. Then, an adaptive algorithm regulates the jet fans performance in order to achieve the target velocity of $1.2\,\mathrm{m.s}^{-1}$ corresponding to the range of values of the air flow velocity in the tunnel required by Slovak regulations [41], i.e., $\langle 1.0\,\mathrm{m.s}^{-1}, 1.5\,\mathrm{m.s}^{-1}\rangle$. If actual air velocity is lower or higher than the target velocity, the jet fans performance increases or decreases significantly, respectively. The RAMP is realized as follows:

$\&RAMP\ ID = \text{'}\ldots\text{'},\ T = 1.15,\ F = 0.80,\ DEVC\_ID = \text{'}\ldots\text{'}\ /$

$\&RAMP\ ID = \text{'}\ldots\text{'},\ T = 1.20,\ F = 0.25\ /$

$\&RAMP\ ID = \text{'}\ldots\text{'},\ T = 1.23,\ F = 0.05\ /$

Every row of the RAMP prescribes the jet fans performance set for the given velocity value. Jet fans performance used by the algorithm for other velocity values is linearly interpolated. The performance of $F = 0.25$ (25 % of the maximal performance) is assigned to the target velocity of $T = 1.20$ (see middle row). The value of F is only estimated; it does not mean that this performance achieves the prescribed target velocity. The precise value of such performance is not known in advance; moreover, it can vary for different phases of fire. The chosen value of F should merely enable algorithm to maintain the prescribed target velocity, otherwise different value must be set. In 12 MW scenarios in sloped tunnel lower value of $F = 0.20$ is used to achieve convergence to the target velocity. The first row of algorithm prescribes significant performance increase $F = 0.80$ if air velocity is slightly lower than the target velocity ($T \leq 1.15$). The last row dampens jet fans performance if actual flow velocity exceeds the target velocity. In 12 MW scenarios in sloped tunnel this row is replaced as follows:

$\&RAMP\ ID = \text{'}\ldots\text{'},\ T = 1.23,\ F = 0.20\ /$

$\&RAMP\ ID = \text{'}\ldots\text{'},\ T = 1.25,\ F = 0.80\ /$

in order to enable algorithm to achieve even negative values of the jet fans velocity necessary for achieving the required target velocity.

The aim of this algorithm is not to model the ventilation control algorithm (Central Control System – CCS) of a real tunnel. Instead, the algorithm in simulations allows very efficient regulation of jet fans, creating the conditions in which ventilation aims are achieved rapidly and then maintaining the air flow velocity very close to the target velocity until the end of simulation. It enables the smoke behaviour examination under intended conditions. The airflow velocity is evaluated at vertical cut, perpendicular to the tunnel axis, which is located at 3 m distance from the left tunnel portal. The mean of all velocities in computational cells of the cut is calculated and used as the main parameter of control algorithm. The choice of the cut located far from the fire ensures that the calculated velocity value corresponds to the flow of the cold air. Therefore, it is not directly affected by the heat of the fire and biased by variable local flows of hot gases in the fire vicinity.

For the three values of HRR and two fire locations, four scenarios are simulated for tunnel as follows:

- S-x-y-0: horizontal (0° slope) without lay-bys,
- S-x-y-0L: horizontal (0° slope) with two lay-bys,
- S-x-y-2: sloped (2° slope) without lay-bys,
- S-x-y-2L: sloped (2° slope) with two lay-bys,

where $x = 3, 5, 12$ correspond to fire HRR and $y = \text{I, II}$ corresponds to fire locations. Therefore, 24 scenarios ($3 \times 2 \times 2 \times 2$) are simulated and evaluated.

The simulations were carried out on the SIVVP cluster at the Institute of Informatics, Slovak Academy of Sciences (Slovakia), which is an IBM dx360 M3 cluster consisting of 54 computational nodes (23 Intel E5645 @ 2.4 GHz CPU, 48 GB RAM); the total number of cores was 648. The nodes are connected by the Infiniband interconnection network with the bandwidth of 40 Gbit/s per link and per direction. Parallel MPI version 6.5.2 of FDS was used. The computational domain is decomposed into 12 meshes of the same dimensions (1 350 000 cells per mesh), each of them assigned to one MPI process (one CPU core). One computational node with 12 cores was used for each simulation; therefore, the total number of 288 computational cores was used for the study.

3 SIMULATION RESULTS AND DISCUSSION

3.1 Ventilation Control Algorithm Evaluation

The air flow velocities averaged for the last 400 s of the simulation are shown in Table 1, demonstrating efficiency of control algorithm and its ability to achieve the target velocity. As it will be shown later, the jet fans velocities vary in time significantly in particular fire scenarios. However, time-averaged air flow velocity created by the jet fans fulfil requirements, reaching the value of $1.2\,\text{m.s}^{-1}$ with the deviation of approximately $0.01\,\text{m.s}^{-1}$ or less in each tested scenario. The deviation is negligible for practical purposes, where the accuracy of approximately tenths of

$m.s^{-1}$ is usually considered. Nevertheless, the air flow velocity is not constant during the course of fire scenarios, as the algorithm responds to dynamics conditions created by developing fires and by heat transfer they create. Table 1 shows the minimal and maximal values of the air flow velocity achieved during the fire scenarios as well as the difference between them. In almost all tested scenarios this difference is below $0.06\,m.s^{-1}$, which is consistent with defined fire ventilation aims. In four scenarios with 12 MW fire in sloped tunnel, the difference achieves the value of almost $0.1\,m.s^{-1}$. However, it is still smaller deviation than can be expected in real conditions, provided by a limited number of anemometers in the tunnel and the large time steps at which their measurements are evaluated. It can be concluded that the control algorithm achieved defined ventilation aims and the smoke movement and stratification can be examined and evaluated under intended conditions.

Simulation	Location I ($y = $ I)				Location II ($y = $ II)			
	Vel	Min	Max	Diff	Vel	Min	Max	Diff
S-3-y-0	1.19	1.18	1.20	0.02	1.19	1.18	1.20	0.02
S-3-y-0	1.20	1.17	1.24	0.07	1.19	1.18	1.20	0.02
S-3-y-2	1.20	1.19	1.22	0.03	1.20	1.19	1.21	0.02
S-3-y-2L	1.20	1.19	1.22	0.03	1.20	1.19	1.22	0.02
S-5-y-0	1.19	1.18	1.21	0.04	1.19	1.18	1.20	0.02
S-5-y-0L	1.19	1.18	1.20	0.02	1.19	1.18	1.22	0.04
S-5-y-2	1.20	1.19	1.22	0.03	1.21	1.19	1.23	0.04
S-5-y-2L	1.20	1.19	1.22	0.03	1.21	1.19	1.23	0.04
S-12-y-0	1.19	1.17	1.22	0.05	1.19	1.17	1.22	0.05
S-12-y-0L	1.19	1.17	1.23	0.06	1.19	1.17	1.23	0.06
S-12-y-2	1.21	1.16	1.26	0.10	1.21	1.16	1.25	0.09
S-12-y-2L	1.21	1.16	1.24	0.09	1.21	1.16	1.25	0.10

Table 1. The air flow velocities averaged for the last 400 s (Vel), minimal (Min) and maximal (Max) air flow velocities achieved during ventilation operation and the difference between maximal and minimal air flow velocities for particular scenarios (Diff)

3.2 Smoke Spread and Stratification

3.2.1 Main Tendencies of Fire Spread

The main features of smoke propagation are very similar for all tested scenarios (Figure 2). A dense smoke layer is formed above the fire under the tunnel ceiling spreading in both directions. The downstream smoke spread is faster, being accelerated by the tunnel jet fans operation. Smoke movement in both directions increases with the increasing fire HRR, supported by a bigger amount of hot smoke. Therefore, the length of backlayering increases with the increasing HRR. The higher tunnel slope, on the other hand, decreases the length of backlayering due to buoyancy forces suppressing backlayering, while the downstream smoke spread is accelerated

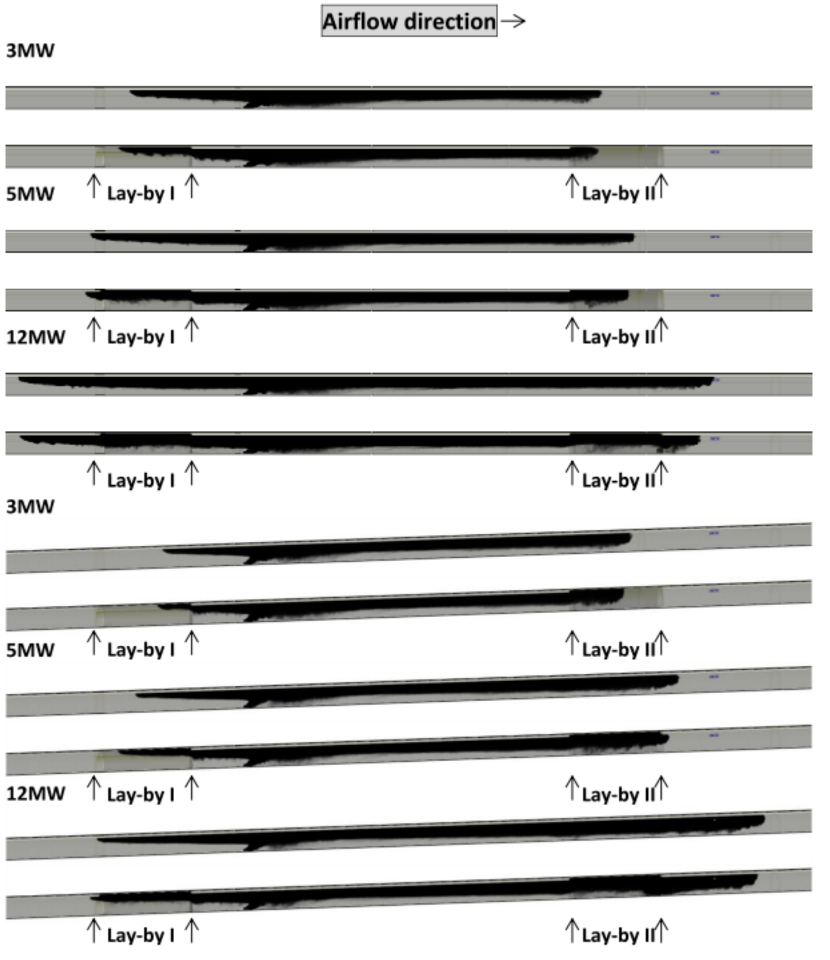

Figure 2. Smoke movement for all fire scenarios with the Fire location II after 120 s to the fire

significantly. The presence of lay-bys influences the fire spread in a more complicated way. The upstream Lay-by I slightly accelerates the upstream smoke spread. The smoke is contained in the lay-by where its rear vertical wall prevents the smoke propagation downstream [38]. Therefore, a larger amount of smoke being cumulated in the lay-by increases the length of backlayering, which is longer than in scenarios without lay-bys.

The downstream smoke spread is decelerated by the Lay-by II, as the upward movement of smoke in the lay-by, caused by its higher ceiling, contributes to the breaking of stratification, and the spread of cooled smoke is slowed down. This effect is less pronounced for well stratified hot smoke, i.e., for 12 MW scenarios and the Fire location I.

3.2.2 Smoke Visibility in Front of the Lay-by II

There can be 2 types of the smoke propagation patterns in the Lay-by II and its vicinity found in the investigated scenarios. The first group includes the patterns caused by the tunnel slopes, which were investigated in [42, 43]. The second group consists of patterns caused by the influence of the lay-bys, analysed in [37, 38]. One of these groups, or their combination, predominates in particular simulations examined in this work.

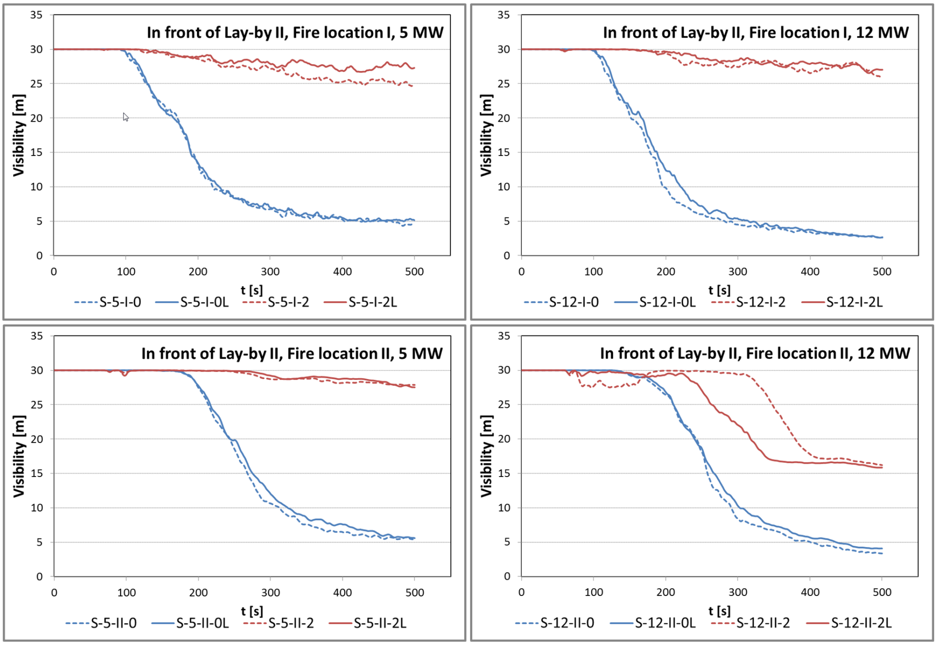

Figure 3. Averaged visibility at head level in front of the area where the Lay-by II is located for 5 MW and 12 MW scenarios

Smoke visibilities at head level in front of the lay-by in 5 MW and 12 MW scenarios are shown in Figure 3. As the smoke visibilities in 3 MW scenarios are similar to 5 MW scenarios, we do not present them. Note that 3 MW scenarios were discussed in [37] more in detail; discussing mainly the differences between 5 and 12 MW scenarios enables to demonstrate the considerable influence of increasing HRR more clearly.

In the case of fires in horizontal tunnels, the smoke behaviour is given almost exclusively by the patterns typical for horizontal tunnels as observed in [42], with only slight influence of other factors. The decrease in visibility starts behind the fire and the region with low visibility expands downstream. It causes that for both 5 and 12 MW fires the visibility decrease occurs earlier in the scenarios with the Fire location I, as the Fire location I is closer to the lay-by than the Fire location II.

In the sloping tunnel scenarios, the decrease in visibility is very small for 5 MW scenarios due to higher buoyancy. The same applies also for the case of 12 MW fire and the Fire location I. However, in 12 MW scenarios for the Fire location II, the decrease in visibility is much more pronounced. This is in line with [43], as in the case of sloping tunnel the area of reduced visibility is created by the counter current of cold air flowing through the right tunnel portal, extending against the direction of the air flow towards the fire. The area spreads more rapidly for the Fire location II as its larger distance from the portal decreases the smoke layer temperature which leads to the more significant entrainment. The influence of the lay-by is manifested in this scenario as well, as the impact of smoke layer into the vertical wall at the end of the lay-by reduces the visibility in the lay-by scenario even more.

3.2.3 Smoke Visibility in the Lay-by II

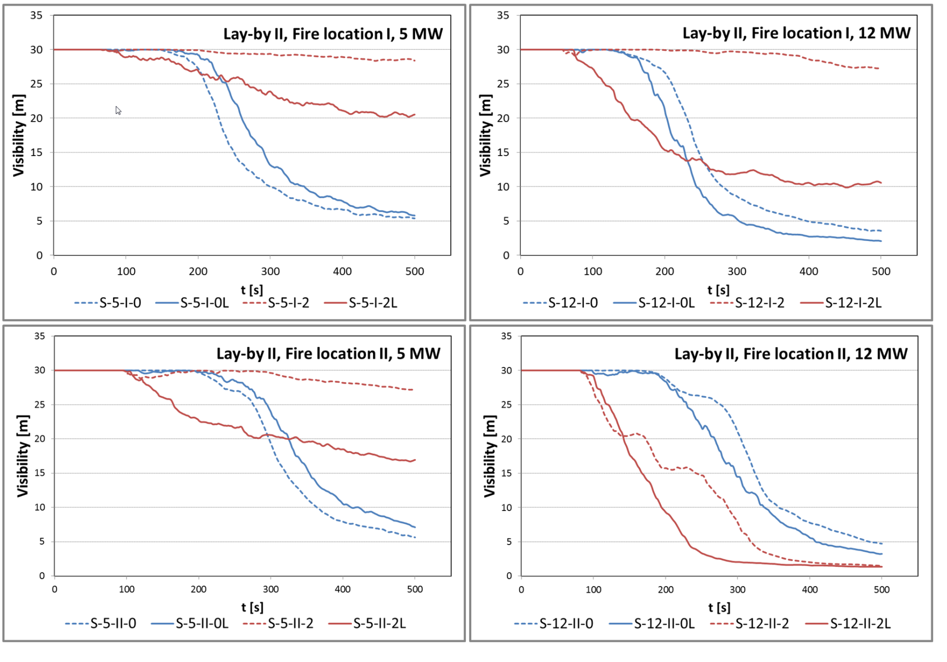

Figure 4. Averaged visibility at head level in the area where the Lay-by II is located for 5 MW and 12 MW scenarios

Smoke visibilities at head level in the Lay-by II in 5 MW and 12 MW scenarios are shown in Figure 4. Smoke spread tendencies in the lay-by are similar to the tendencies in front of the lay-by.

In the case of fires in horizontal tunnels, decrease in visibility occurs earlier for the Fire location I than for the Fire location II. It is consistent with [42] as well as with the observation in front of the lay-by. However, the differences between lay-by and non-lay-by scenarios are more significant. In the case of 5 MW scenarios, there is slightly better visibility in the lay-by scenario as a consequence of presence of the raised lay-by ceiling under which well-stratified smoke flows. In 12 MW fire scenarios, in contrast to 5 MW scenarios, visibility is lower in the lay-by scenarios case. This is due to the thicker layer of smoke under the lay-by ceiling and faster impact of smoke layer into the vertical wall at the end of the lay-by.

In the case of 5 MW scenarios in sloping tunnel, on the other hand, there is a more significant decrease in visibility in the lay-by scenarios, due to the impact of fast-flowing smoke hitting the vertical wall at the end of the lay-by. Nevertheless, significantly better visibility is maintained in 5MW sloping scenarios than in the horizontal scenarios due to buoyancy maintaining smoke stratification.

Considerable differences between lay-by and non-lay-by scenarios are manifested also in the case of 12 MW fire in sloping tunnels. For the Fire location I, buoyance keeps almost perfect visibility in the case of tunnel without lay-bys, while in the case of lay-by scenario, on the contrary, the visibility decreases even more than in 5 MW case due to the impact of smoke layer hitting the vertical wall at the end of the lay-by. For the Fire location II, the visibility drop in the lay-by is extraordinarily significant in both cases, which is similar to the smoke behaviour in front of the lay-by caused by the same mechanism.

3.2.4 Smoke Visbility Behind the Lay-by II

Smoke visibilities at head level behind the Lay-by II in 5 MW and 12 MW scenarios are shown in Figure 5.

In the case of fire in horizontal tunnel, the smoke behaviour pattern is again given by the tendency of visibility decrease in fire vicinity earlier, for both 5 and 12 MW fires. In contrast to the situation in front of the lay-by and in the lay-by, this time the spread of smoke is significantly affected by its spread through the lay-by, and thus the decrease in visibility is more pronounced in the lay-by scenarios.

For 5 MW fire in the sloping tunnel without lay-bys, the decrease in visibility is minimal regardless of the fire location. However, the lay-by causes a significant decrease in visibility, which is more pronounced for the more distant Fire location II as the smoke reaching the lay-by level is significantly colder. The same applies to the case of 12 MW lay-by scenarios. In the 12 MW non-lay-by scenario for the Fire location I, the smoke is hotter and thus slightly better stratified than in the case of the Fire location II. Perfect visibility is maintained until the 300 s to the fire, when the visibility is rapidly reduced by scattered smoke brought by the cold counter current. This effect is even more pronounced for the Fire location II. Visibility drop

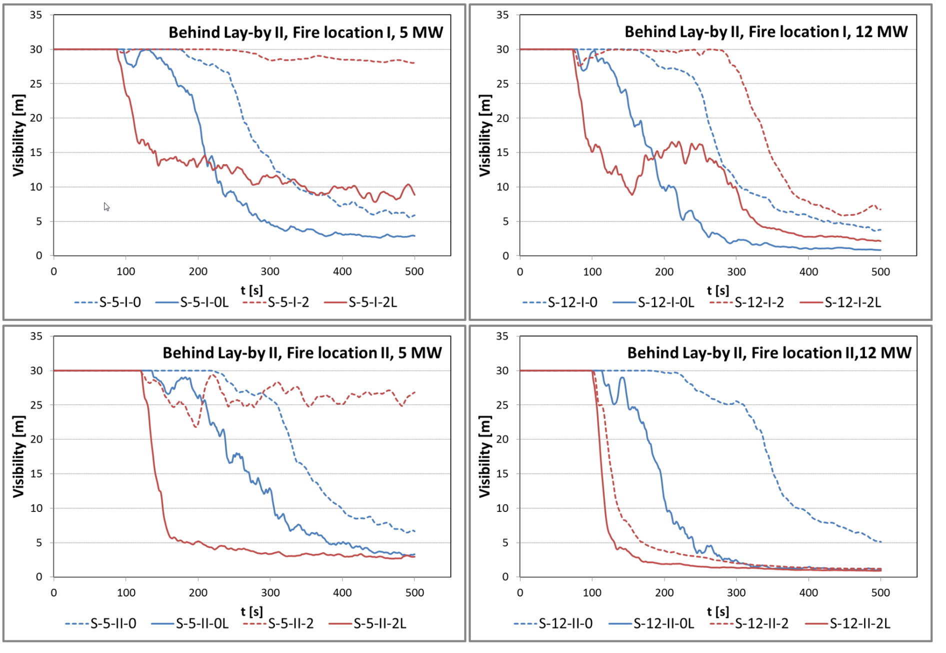

Figure 5. Averaged visibility at head level behind the area where the Lay-by II is located for 5 MW and 12 MW scenarios

caused by the cold counter current is so considerable for the Fire location II that the lay-by causes only its minimal additional deterioration.

3.3 Simulation Efficiency

The aim of the algorithm used to regulate the jet fans performance in different fire scenarios is to achieve the required air flow velocity under different conditions. The resulting jet fans velocity varies for each scenario and its value is the main factor that affects the simulation elapsed time. In order to illustrate similarities between tested scenarios, the 5 s moving averages of the jet fans velocities, recorded in simulations in 1 s frequency, are shown in Figure 6. In Table 2, averages of the jet fans velocities for the last 400 s of the simulation and the simulation elapsed times are shown.

For the pairs of scenarios that differ only in the existence or non-existence of the lay-bys, the values of the averaged jet fans velocity $\overline{v_{jet}}$ and simulation elapsed time are relatively close, with $\overline{v_{jet}}$ differences less or equal to 1.1 m.s^{-1}. However, the values for the different pairs are very different. For horizontal tunnel, the jet fans velocity required to achieve the target air flow velocity increases with increasing HRR, as the ventilation must overcome bigger buoyancy induced by increasing fire HRR (see Figure 6). Conversely, for sloping tunnel, the dependence is reversed, i.e.,

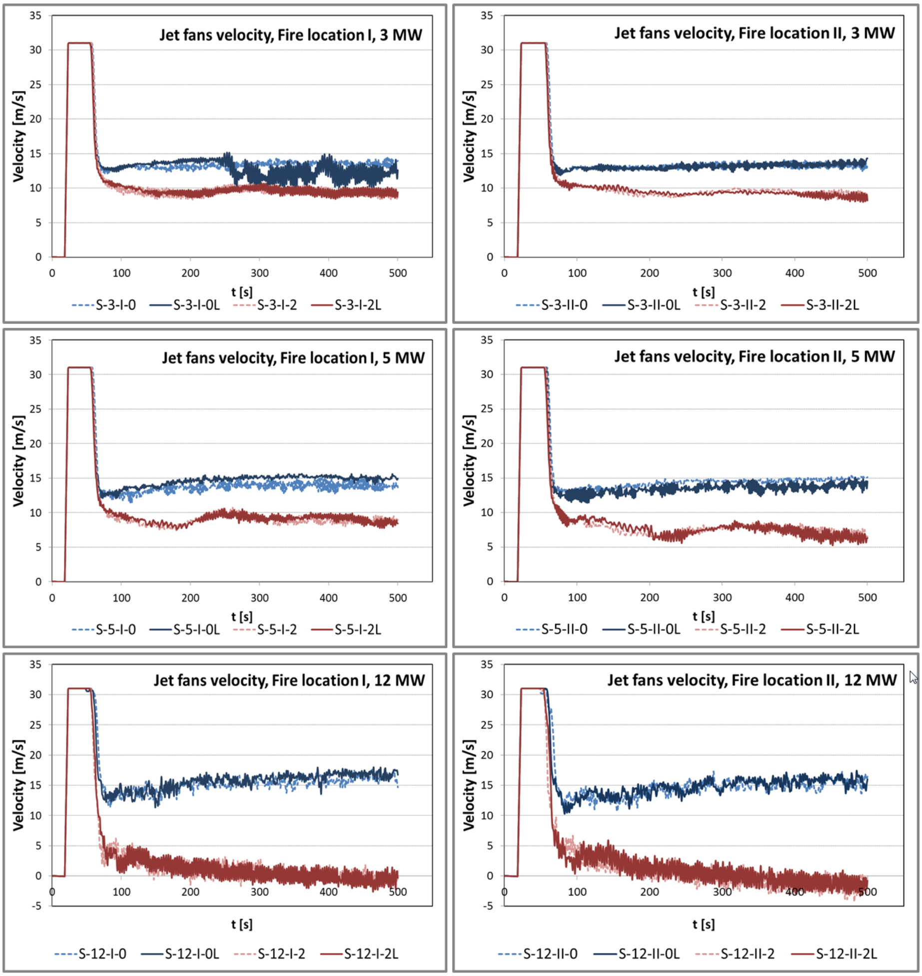

Figure 6. 5 s moving averages of jet fans velocities of tested scenarios

the jet fans velocity decreases with increasing HRR. This is because of the buoyancy induced by fire due to the inclination of the tunnel which speeds up the air flow in the tunnel and enhances the ventilation effect. Therefore, a significantly lower jet fans velocity is sufficient to achieve the required target air flow velocity. For 12 MW HRR the jet fans performance even goes into negative values in some phases of the fire, slowing down the air flow. Therefore, increasing HRR and tunnel slope change the course of simulations significantly.

The jet fans velocity is the highest value of velocity within the computational domain and it is therefore decisive for determination of the numerical time step of FDS simulation. As the jet fans velocity increases, the time step decreases and

Simulation	Location I (y=I)			Location II (y=II)		
	$\overline{v_{jet}}$	*Time*	*Dev*	$\overline{v_{jet}}$	*Time*	*Dev*
S-3-y-0	13.3	355	2.0	13.2	362	2.0
S-3-y-0	12.8	340	4.1	13.2	351	2.1
S-3-y-2	9.5	269	2.5	9.4	208	0.7
S-3-y-2L	9.5	269	2.2	9.4	204	0.8
S-5-y-0	13.7	417	2.3	14.4	357	0.9
S-5-y-0L	14.8	353	1.1	13.5	410	2.3
S-5-y-2	8.9	279	1.7	7.4	263	1.6
S-5-y-2L	9.0	272	1.6	7.5	256	1.8
S-12-y-0	15.3	599	2.2	14.6	593	2.3
S-12-y-0L	15.8	516	2.4	14.8	570	2.5
S-12-y-2	0.8	993	5.6	0.1	1 018	5.6
S-12-y-2L	0.7	965	5.7	0.5	997	5.6

Table 2. Averaged jet fans velocities, $\overline{v_{jet}}$ [m.s^{-1}], simulation elapsed times, *Time* [hrs] and average deviations of jet fans velocities, *Dev* [m.s^{-1}]

the elapsed time increases. It is necessary to take into account not only the averaged value of the jet fans velocity, $\overline{v_{jet}}$, but also its time fluctuations, *Dev* (see Table 2). The used jet fans control algorithm does not allow achieving stable jet fans performance. The performance fluctuates permanently and only its averaged value allows reaching the desired target velocity. The highly fluctuating jet fans performance causes changes of the value of the time step and disrupts simple dependence between $\overline{v_{jet}}$ and elapsed time. Especially for the 12 MW fire in sloping tunnel, both the deviation and elapsed time values are extremely high, significantly higher than would be expected based on the values observed in the other scenarios.

The values of jet fans velocities $\overline{v_{jet}}$ against elapsed times of particular scenarios are shown in Figure 7. The simulations can be divided into four groups. Three groups are characterized by growing dependence between jet fans velocity and elapsed time, as it is manifested by the trend line in Figure 7. The first group with the smallest values of elapsed time (significantly less than 300 hours) consists of the simulations of less intensive fires (3 and 5 MW) in sloping tunnels. The second group consists of the simulations of less intensive fires in horizontal tunnels. The elapsed time varies between 340 and 417 hours for these simulations. 12 MW scenarios in horizontal tunnels are included in the third group with the significantly longer elapsed times (516–599 hours). The fourth group of 12 MW fire simulations in sloping tunnel is specific and the growing dependence between jet fans velocity and elapsed time does not appear here. Although elapsed times are extremely long (about 1 000 hours), $\overline{v_{jet}}$ velocities are close to zero. The long time step of these simulations is probably set by FDS due to significant variability of the air flow velocity during the simulations. Although the differences between Max and Min values for the forth group in Figure 7 are not significantly higher than corresponding dif-

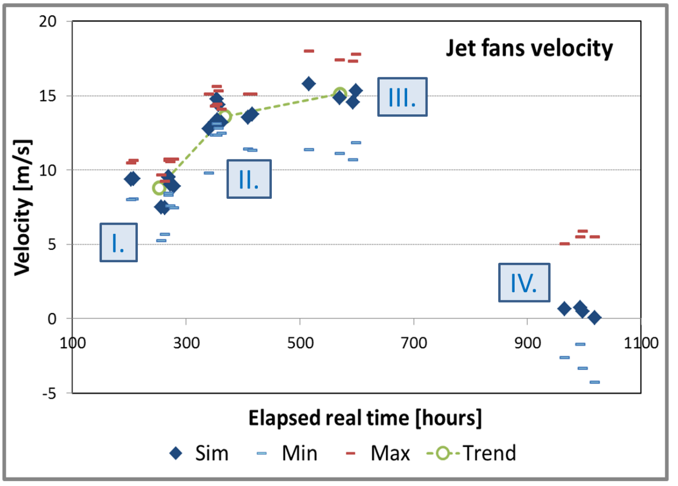

Figure 7. Four groups of simulations, characterised by the jet fans velocities, $\overline{v_{jet}}$, and elapsed times: Min and Max determine the highest and the lowest jet fans velocities, respectively, observed during simulation, Trend represents the trend line connecting averages of the $\overline{v_{jet}}$ and elapsed times of simulations forming the given group

ferences for the other three groups, average deviations of jet fans velocities for the simulations in the fourth group are significantly higher than corresponding deviation for the other groups, as can be seen in Table 2. Moreover, deviations of the air flow velocities in the fourth group simulations are extraordinary high as well (see Table1).

The influence of lay-bys and fire locations on the averaged jet fans velocity $\overline{v_{jet}}$ and the elapsed time is different for horizontal and sloping tunnels (see Table 2).

The dependence is simpler in the case of sloping tunnels. The $\overline{v_{jet}}$ velocity for the Fire location II is lower than for the Fire location I during most of the simulation due to a larger amount of hot smoke contained in the tunnel for the Fire location II. Bigger buoyancy of the smoke increases air flow velocity, decreasing the necessary jet fans performance. Correspondingly, elapsed times are usually lower for the Fire location II, although their decrease is less pronounced than the decrease of jet fans velocity. In the case of 12 MW fires, the elapsed times are slightly higher the for the Fire location II in spite of lower jet fans velocity, probably due to significant velocity fluctuations in the scenarios. The effect of the tunnel lay-bys on monitored quantities seems to be negligible and only random (see Table 2).

The simulations of the horizontal tunnels scenarios do not indicate the significant systematic influence of the fire location and lay-bys on the averaged jet fans velocity $\overline{v_{jet}}$ nor the elapsed time. The observed deviations of monitored quantities seem to be random (see Table 2). Out of the total of 6 pairs of scenarios with the different fire location, the $\overline{v_{jet}}$ value is higher in four of them for the Fire location I, while it is higher in two of them for the Fire location II. Out of the total of 6 pairs of the lay-bys and non-lay-bys scenarios, the $\overline{v_{jet}}$ value is higher in three of them for the lay-bys scenarios and in three of them for the non-lay-bys scenarios. Some observed average velocity differences within the tested pairs achieve significant values up to 1.1m.s^{-1}. Such complex behaviour can be caused by mutual interaction of several factors, including the different volume of air in tunnels with and without lay-bys, interaction of air flow in the tunnel with the smoke layer in complicated lay-by geometry as well as the influence of internal settings of FDS related to the time step determination. The probability of the latter influence is supported by the fact that out of the total of 12 evaluated pairs, in 9 pairs the scenario with higher $\overline{v_{jet}}$ has lower elapsed time. However, this effect on elapsed time is considerably smaller than the tendency shown in Figure 7.

4 CONCLUSIONS

Parametric study consisted of 24 simulations of tunnel fire was performed on the HPC SIVVP cluster by well-known code FDS, version 6.5.2, to investigate the influence of selected tunnel and fire parameters on smoke stratification and the simulation elapsed time. Three values of fire heat release rate (3, 5 and 12 MW) for two different fire locations (in the middle between the lay-bys and near the first lay-by) and two tunnel slopes ($0°$ and $2°$), as well as a presence or non-presence of two lay-bys at specified locations in the tunnel were taken into consideration. The geometry and equipment of the considered 900 m long tunnel is similar to the bi-directional motorway tunnel Polana with horseshoe cross-section, two emergency lay-bys and longitudinal ventilation which is in operation in Slovakia. Each simulation was performed as a 12-mesh fire simulation using 12 MPI processes assigned to 12 CPU cores of one compute cluster node. The total number of cluster cores used for the whole parametric study was 288.

The analysis has been focused on smoke stratification in the downstream lay-by and in its vicinity. Visibility in the tested locations is influenced by a combination of various tendencies of smoke spread:

- In horizontal tunnel, the visibility drop starts in the fire vicinity and the region with low visibility expands downstream towards the lay-by.
- In sloping tunnel, the smoke at head level spreads in opposite direction from the downstream tunnel portal due to entrainment caused by cold air counter current.
- Thicker smoke layer corresponding to bigger HRR enhances the visibility decrease after interaction with the lay-by geometry.
- Higher lay-by ceiling generally improves local visibility in the lay-by, while the impact of fast-flowing smoke hitting the vertical wall at the end of the lay-by causes a significant local decrease of visibility.

- More extensive smoke cooling caused by tunnel walls corresponding to the fire location farther from the lay-by intensifies the visibility decrease in the lay-by especially in sloping tunnels.

Elapsed times of particular simulations are very variable, with 1:5 ratio of the slowest and fastest simulations. The main factor influencing the simulation elapsed time is the jet fans velocity required to achieve the given target velocity intended to maintain stratification in the tunnel. In horizontal tunnel, the jet fans velocity increases with increasing HRR, while in sloping tunnel the jet fans velocity decreases with increasing HRR, as buoyancy accelerates the air flow in the tunnel and a significantly lower jet fans performance is necessary. The numerical time step generally decreases for higher jet fans velocities, which results in longer elapsed times.

In horizontal tunnels scenarios, no systematic influence of the fire location nor lay-bys on the averaged jet fans velocity and elapsed time is observed.

In sloping tunnels scenarios, the jet fans velocity is lower for the fire location closer to the upstream tunnel portal since a certain moment due to buoyancy of larger amount of hot smoke accumulated in the tunnel. However, the influence of the jet fans velocity on the elapsed time is less pronounced in this case. The effect of lay-bys on the monitored quantities in sloping tunnel is negligible and seems to be only random.

The results of this paper may help to understand some specific tendencies of fire smoke spread in real road tunnels and also the factors that determine the elapsed time required for simulation of tunnel fire scenarios. They may also contribute to the improvement of tunnel fire scenarios design and to more efficient use of available computational resources.

Acknowledgment

The authors would like to thank Peter Schmidt (National Motorway Company, Slovakia) for technical specifications of road tunnels. This work was supported by the Slovak Science Foundation (project No. VEGA 2/0108/20).

REFERENCES

[1] McGrattan, K.—Hostikka, S.—McDermott, R.—Floyd, J.—Weinschenk, C.—Overholt, K.: Fire Dynamics Simulator: Technical Reference Guide (6th Edition). National Institute of Standards and Technology, Gaithersburg, Maryland, USA, and VTT Technical Research Centre of Finland, Espoo, Finland, 2017.

[2] McGrattan, K.—Hostikka, S.—McDermott, R.—Floyd, J.—Weinschenk, C.—Overholt, K.: Fire Dynamics Simulator: User's Guide (6th Edition). National Institute of Standards and Technology, Gaithersburg, Maryland, USA, and VTT Technical Research Centre of Finland, Espoo, Finland, 2017.

[3] McGrattan, K.—Hostikka, S.—McDermott, R.—Floyd, J.—Weinschenk, C.—Overholt, K.: Fire Dynamics Simulator: Technical Reference Guide. Volume 3: Validation (6th Edition). National Institute of Standards and Technology, Gaithersburg, Maryland, USA, and VTT Technical Research Centre of Finland, Espoo, Finland, 2014.

[4] McGrattan, K. B.—Bouldin, C.—Forney, G. P.: Federal Building and Fire Safety Investigation of the World Trade Center Disaster: Computer Simulation of the Fires in the WTC Towers (NIST NCSTAR 1-5F). National Institute of Standards and Technology, Gaithersburg, Maryland, USA, 2005.

[5] Tilley, N.—Rauwoens, P.—Merci, B.: Verification of the Accuracy of CFD Simulations in Small-Scale Tunnel and Atrium Fire Configurations. Fire Safety Journal, Vol. 46, 2011, No. 4, pp. 186–193, doi: 10.1016/j.firesaf.2011.01.007.

[6] Valasek, L.—Glasa, J.: On Realization of Cinema Hall Fire Simulation Using Fire Dynamics Simulator. Computing and Informatics, Vol. 36, No. 4, 2017, pp. 971–1000, doi: 10.4149/cai_2017_4_971.

[7] Zhao, D.—Jiang, J.—Zhou, R.—Tong, Y.—Wu, F.—Shi, L.: Numerical Study on the Optimisation of Smoke Ventilation Mode for Interchange Subway Station Fire. International Journal of Ventilation, Vol. 15, 2016, No. 1, pp. 79–93, doi: 10.1080/14733315.2016.1173294.

[8] Deckers, X.—Haga, S.—Tilley, N.—Merci, B.: Smoke Control in Case of Fire in a Large Car Park: CFD Simulations of Full-Scale Configurations. Fire Safety Journal, Vol. 57, 2013, pp. 22–34, doi: 10.1016/j.firesaf.2012.02.005.

[9] Heinisuo, M.—Partanen, M.: Modeling of Car Fires with Sprinklers. Research Report 161. Tampere University of Technology, Department of Civil Engineering, Structural Engineering. Tampere, Finland, 2013.

[10] Weisenpacher, P.—Glasa, J.—Halada, L.: Parallel Computation of Smoke Movement During a Car Park Fire. Computing and Informatics, Vol. 35, No. 6, 2016, pp. 1416–1437.

[11] Fernández-Alaiz, F.—Castañón, A. M.—Gómez-Fernández, F.—Bascompta, M.: Mine Fire Behavior under Different Ventilation Conditions: Real-Scale Tests and CFD Modeling. Applied Sciences, Vol. 10, 2020, No. 10, doi: 10.3390/app10103380.

[12] Weisenpacher, P.—Glasa, J.—Halada, L.: Automobile Interior Fire and Its Spread to an Adjacent Vehicle: Parallel Simulation. Journal of Fire Sciences, Vol. 34, 2016, No. 4, pp. 305–322, doi: 10.1177/0734904116647972.

[13] Chapman, B.—Jost, G.—van der Pas, R.: Using OpenMP: Portable Shared Memory Parallel Programming. The MIT Press, Cambridge, Massachusetts, 2007.

[14] Gropp, W.—Lusk, E.—Skjellum, A.: Using MPI: Portable Parallel Programming with the Message-Passing Interface. 2nd Edition. The MIT Press, Cambridge, Massachusetts, 1999.

[15] Klote, J. H.—Milke, J. A.: Design of Smoke Management Systems. American Society of Heating, Refrigerating and Air Conditioning Engineers, Inc., Atlanta, Georgia, USA, 1992.

[16] Boehm, M.—Fournier, L.—Truchot, B.: Smoke Stratification Stability: Pre-

sentation of Experiments. Proceedings of 4th International Conference on Tunnel Safety and Ventilation, 2008, pp. 176–182.

[17] Ingason, H.—Li, Y. Z.—Lönnermark, A.: Smoke Stratification. In: Tunnel Fire Dynamics. Springer, New York, NY, 2015, pp. 321–332, doi: 10.1007/978-1-4939-2199-7_12.

[18] Al-Waked, R.—Nasif, M.—Groenhout, N.—Partridge, L.: Natural Ventilation of Residential Building Atrium under Fire Scenario. Case Studies in Thermal Engineering, Vol. 26, 2021, Art. No. 101041, doi: 10.1016/j.csite.2021.101041.

[19] Huang, D. F.—Li, S. C.: An Experimental Investigation of Stratification Characteristic of Fire Smoke in the Corridor under the Effect of Outdoor Wind. Journal of Wind Engineering and Industrial Aerodynamics, Vol. 179, 2018, pp. 173–183, doi: 10.1016/j.jweia.2018.05.021.

[20] Li, D.—Zhu, G.—Zhu, H.—Yu, Z.—Gao, Y.—Jiang, X.: Flame Spread and Smoke Temperature of Full-Scale Fire Test of Car Fire. Case Studies in Thermal Engineering, Vol. 10, 2017, pp. 315–324, doi: 10.1016/j.csite.2017.08.001.

[21] Hu, L. H.—Fong, N. K.—Yang, L. Z.—Chow, W. K.—Li, Y. Z.—Huo, R.: Modeling Fire-Induced Smoke Spread and Carbon Monoxide Transportation in a Long Channel: Fire Dynamics Simulator Comparisons with Measured Data. Journal of Hazardous Materials, Vol. 140, 2007, No. 1-2, pp. 293–298, doi: 10.1016/j.jhazmat.2006.08.075.

[22] Chen, Y. J.—Shu, C. M.—Ho, S. P.—Kung, H. C.—Chien, S. W.—Ho, H. H.—Hsu, W. S.: Analysis of Smoke Movement in the Hsuehshan Tunnel Fire. Tunnelling and Underground Space Technology, Vol. 84, 2019, pp. 142–150, doi: 10.1016/j.tust.2018.11.007.

[23] Hsu, W. S.—Huang, Y. H.—Shen, T. S.—Cheng, C. Y.—Chen, T. Y.: Analysis of the Hsuehshan Tunnel Fire in Taiwan. Tunnelling and Underground Space Technology, Vol. 69, 2017, pp. 108–115, doi: 10.1016/j.tust.2017.06.011.

[24] Ang, C. D.—Rein, G.—Peiro, J.—Harrison, R.: Simulating Longitudinal Ventilation Flows in Long Tunnels: Comparison of Full CFD and Multi-Scale Modelling Approaches in FDS6. Tunnelling and Underground Space Technology, Vol. 52, 2016, pp. 119–126, doi: 10.1016/j.tust.2015.11.003.

[25] Brzezinska, D.—Sompolinski, M.: The Accuracy of Mapping the Airstream of Jet Fan Ventilators by Fire Dynamics Simulator. Science and Technology for the Built Environment, Vol. 23, 2017, No. 5, pp. 736–747, doi: 10.1080/23744731.2016.1249234.

[26] Brzezinska, D.: Practical Aspects of Jet Fan Ventilation Systems Modelling in Fire Dynamics Simulator Code. International Journal of Ventilation, Vol. 17, 2018, pp. 225–239, doi: 10.1080/14733315.2017.1400733.

[27] Tang, F.—Zhao, Z.—Zhao, K.: Experimental Investigation on Carriage Fires Hazards in the Longitudinal Ventilated Tunnels: Assessment of the Smoke Stratification Features. Safety Science, Vol. 130, 2020, Art. No. 104901, doi: 10.1016/j.ssci.2020.104901.

[28] Yang, D.—Hu, L. H.—Huo, R.—Jiang, Y. Q.—Liu, S.—Tang, F.: Experimental Study on Buoyant Flow Stratification Induced by a Fire in a Horizontal Channel. Applied Thermal Engineering, Vol. 30, 2010, No. 8-9, pp. 872–878, doi:

10.1016/j.applthermaleng.2009.12.019.

[29] Nyman, H.—Ingason, H.: Temperature Stratification in Tunnels. Fire Safety Journal, Vol. 48, 2012, No. 1, pp. 30–37, doi: 10.1016/j.firesaf.2011.11.002.

[30] Guo, Y.—Yuan, Z.—Yuan, Y.—Cao, X.—Zhao, P.: Numerical Simulation of Smoke Stratification in Tunnel Fires under Longitudinal Velocities, Underground Space, Vol. 6, 2021, No. 2, pp. 163–172, doi: 10.1016/j.undsp.2019.11.001.

[31] Deng, T.—Norris, S.—Sharma, R. N.: Numerical Investigation on the Stability of Tunnel Smoke Stratification under the Effect of Water Spray and Longitudinal Ventilation. Tunnelling and Underground Space Technology, Vol. 112, 2021, Art. No. 103901, doi: 10.1016/j.tust.2021.103901.

[32] Gannouni, S.—Zinoubi, J.—Ben Maad, R.: Numerical Study on the Thermal Buoyant Flow Stratification in Tunnel Fires with Longitudinal Imposed Airflow: Effect of an Upstream Blockage. International Journal of Thermal Sciences, Vol. 136, 2019, pp. 230–242, doi: 10.1016/j.ijthermalsci.2018.10.041.

[33] Rattei, G.: Safety Installations in Road Tunnels – Are They Used in Incident Cases? Proceedings of 5th International Conference on Tunnel Safety and Ventilation, Graz, Austria, 2010, pp. 235–241.

[34] Weisenpacher, P.—Valasek, L.: Computer Simulation of Airflows Generated by Jet Fans in Real Road Tunnel by Parallel Version of FDS 6. International Journal of Ventilation, Vol. 20, 2021, No. 1, pp. 20–33, doi: 10.1080/14733315.2019.1698164.

[35] Pospisil, P.—Ockajak, R.: Tunel Poľana – DRS vetranie tunela a únikovej štôlne [Polana Tunnel – Tunnel and Escape Tunnel Ventilation]. Technical Report. IP Engineering GmbH, Munchenstein, Switzerland, 2016 (in Slovak).

[36] Pospisil, P.—Ockajak, R.: Skúšky vetrania tunela Poľana a Svrčinovec [Ventilation Tests in Polana and Svrcinovec Tunnels]. Technical Report. IP Engineering GmbH, Munchenstein, Switzerland, 2017 (in Slovak).

[37] Weisenpacher, P.—Glasa, J.—Valasek, L.: Influence of Emergency Lay-Bys on Smoke Stratification in Case of Fire in Bi-Directional Tunnel: Parallel Simulation. Proceedings of the 31st European Modeling and Simulation Symposium (EMSS 2019), 2019, pp. 47–53, doi: 10.46354/i3m.2019.emss.009.

[38] Weisenpacher, P.—Glasa, J.—Valasek, L.—Kubisova, T.: FDS Simulation of Smoke Backlayering in Emergency Lay-By of a Road Tunnel with Longitudinal Ventilation. Journal of Physics: Conference Series, Vol. 2090, 2021, Art. No. 012100, doi: 10.1088/1742-6596/2090/1/012100.

[39] Danišovič, P.—Šrámek, J.—Hodoň, M.—Húdik, M.: Testing Measurements of Airflow Velocity in Road Tunnels. RSP 2017 – XXVI R-S-P Seminar 2017 Theoretical Foundation of Civil Engineering. MATEC Web of Conferences, Vol. 117, 2017, Art. No. 00035, doi: 10.1051/matecconf/201711700035.

[40] Sirilla, M.—Schmidt, P.: D3 Žilina (Strážov) – Žilina (Brodno), Považský Chlmec Tunnel. Inžinierske Stavby, Vol. 65, 2017, No. 6, pp. 30–33 (in Slovak).

[41] NDS: Technické podmienky TP 049 – Vetranie cestných tunelov [Technical Conditions TP 049 – Road Tunnels Ventilation]. Ministry of Transport and Construction, NDS, Bratislava, Slovak Republic, 2018 (in Slovak).

[42] Weisenpacher, P.—Glasa, J.—Valasek, L.: Computer Simulation of Smoke Stratification During Fire in Bi-Directional Road Tunnel by FDS 6. Proceedings of the MCS-10: Tenth Mediterranean Combustion Symposium, Naples, Italy, 2017.

[43] Weisenpacher, P.—Glasa, J.—Valasek, L.: Influence of Slope and External Temperature on Smoke Stratification in Case of Fire in Bi-Directional Road Tunnel. AMCSE 2017 – International Conference on Applied Mathematics, Computational Science and Systems Engineering. ITM Web of Conferences, Vol. 16, 2018, Art. No. 02002, doi: 10.1051/itmconf/20181602002.

Peter Weisenpacher studied theoretical physics at the Comenius University, Faculty of Mathematics and Physics, Department of Theoretical Physics, Bratislava, Slovakia and received his Ph.D. degree in 2003. He works as Senior Scientist at the Slovak Academy of Sciences, Institute of Informatics, Department of Parallel Computational Methods and Algorithms. His current research interests include computational fluid dynamics, fire computer simulation and parallel computing. He participates in various research projects on fire simulation.

Lukas Valasek graduated in applied mathematics in 2012, received his Eng. degree in mathematical and computer modelling at the Slovak University of Technology in Bratislava, Faculty of Civil Engineering and his Ph.D. degree in applied informatics at the Slovak University of Technology in Bratislava, Faculty of Informatics and Information Technologies. He works for the Institute of Informatics, Slovak Academy of Sciences in Bratislava. His major research interests include mathematical modelling and computer simulation of fires and their consequences.

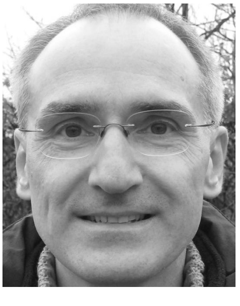

Jan Glasa graduated in numerical mathematics in 1986 and received his R.N.Dr. (Rerum Naturalium Doctor) degree in numerical mathematics and optimization methods and algorithms at the Comenius University in Bratislava, Slovakia and his Candidate of Sc. degree (equivalent to a Ph.D.) in computer science at the Slovak Academy of Sciences. He works for the Institute of Informatics, Slovak Academy of Sciences in Bratislava as Senior Scientist. His current research interests include mathematical modelling and computer simulation of fires and parallel computing.